Title

Krüppel-Like Factor 4 Regulation of Cholesterol-25-Hydroxylase and Liver X Receptor Mitigates Atherosclerosis Susceptibility

Journal

Circulation, 136(14)

ISSN

0009-7322

Authors

Li, Zhao
Martin, Marcy
Zhang, Jin
et al.

Publication Date

2017-10-03

DOI

10.1161/circulationaha.117.027462

Peer reviewed

Published in final edited form as:

Circulation. 2017 October 03; 136(14): 1315–1330. doi:10.1161/CIRCULATIONAHA.117.027462.

KLF4 Regulation of Ch25h and LXR Mitigates Atherosclerosis Susceptibility

Zhao Li, BS[1,2,*], **Marcy Martin, BS**[3,5,*], **Jin Zhang, BS**[1,2], **Hsi-Yuan Huang, PhD**[6], **Liang Bai, PhD**[1,2], **Jiao Zhang, MD**[1,2,3], **Jian Kang, PhD**[3], **Ming He, MD, PhD**[1,2,3], **Jie Li, BS**[1,2], **Mano R. Maurya, PhD**[4], **Shakti Gupta, PhD**[4], **Guangjin Zhou, PhD**[7], **Panjamaporn Sangwung, PhD**[7], **Yong-Jiang Xu, PhD**[3], **Ting Lei, PhD**[1,2], **Hsien-Da Huang, PhD**[6], **Mohit Jain, MD**[3], **Mukesh K. Jain, MD**[7], **Shankar Subramaniam, PhD**[4], and **John Y-J. Shyy, PhD**[1,2,3]

[1]Cardiovascular Research Center, School of Basic Medical Sciences, Xi'an Jiaotong University Health Science Center, Ministry of Education of China, Xi'an, 710061, China

[2]Key Laboratory of Environment and Genes Related to Diseases, Xi'an Jiaotong University, Ministry of Education of China, Xi'an, 710061, China

[3]Division of Cardiology, Department of Medicine, University of California, San Diego, La Jolla, CA 92093

[4]Department of Bioengineering, University of California, San Diego, La Jolla, CA 92093

[5]Division of Biochemistry and Molecular Biology, University of California, Riverside, Riverside, CA 92521

[6]Institute of Bioinformatics and Systems Biology and Department of Biological Science and Technology, National Chiao Tung University, Hsin-Chu, 300, Taiwan

[7]Department of Medicine, Case Western Reserve University School of Medicine, Cleveland, OH 44106

Abstract

Background—Atherosclerosis is a multifaceted inflammatory disease involving cells in the vascular wall [e.g., endothelial cells (ECs)] as well as circulating and resident immunogenic cells (e.g., monocytes/macrophages). Acting as a ligand for liver X receptor (LXR), but an inhibitor of sterol regulatory element binding protein 2 (SREBP2), 25-hydroxycholesterol (25-HC) and its catalyzing enzyme cholesterol-25-hydroxylase (Ch25h) are important in regulating cellular inflammatory status and cholesterol biosynthesis in both ECs and monocytes/macrophages.

To whom correspondence should be addressed: John Y-J. Shyy: Cardiovascular Research Center, Xi'an Jiaotong University Health Science Center, 76 Yanta West Road, Xi'an, Shaanxi, 710061, China; Department of Cardiology, School of Medicine, University of California, San Diego, 9500 Gilman Dr., La Jolla, CA 92093, USA, Fax: 858-822-3027, Tel: 858-534-3736, jshyy@ucsd.edu.
*Authors contributed equally

Author Contributions

Z.L., M. Martin, and J.Y.S designed research; Z.L., M. Martin, Jin Z., L.B., Jiao Z., J.K., M.H., J.L., G.Z., P.S., and Y.X., performed research; Z.L., M. Martin, H.Y.H., M. Maurya, S.G., T.L., H.D.H., M.J, M.K.J., S.S., and J.Y.S. analyzed data; M. Martin, Z.L., and J.Y.S wrote and edited the manuscript.

Disclosures

None.

Methods—Bioinformatic analyses were used to investigate RNA-seq data to identify cholesterol oxidation and efflux genes regulated by KLF4. *In vitro* experiments involving cultured ECs and macrophages and *in vivo* methods involving mice with Ch25h ablation were then used to explore the atheroprotective role of KLF4-Ch25h/LXR.

Results—Vasoprotective stimuli increased the expression of Ch25h and LXR via krüppel-like factor 4 (KLF4). The KLF4-Ch25h/LXR homeostatic axis functions through suppressing inflammation, evidenced by the reduction of inflammasome activity in ECs and the promotion of M1 to M2 phenotypic transition in macrophages. The increased atherosclerosis in ApoE$^{-/-}$/Ch25h$^{-/-}$ mice further demonstrates the beneficial role of the KLF4-Ch25h/LXR axis in vascular function and disease.

Conclusions—KLF4 transactivates Ch25h and LXR thereby promoting the synergistic effects between ECs and macrophages to protect against atherosclerosis susceptibility.

Keywords

Endothelial cells; macrophages; shear stress; atherosclerosis; cholesterol metabolism; inflammation

Introduction

Krüppel-like factor 4 (KLF4) is a master transcription factor (TF) regulating the anti-inflammatory phenotype of both vascular endothelial cells (ECs) and monocytes/macrophages. Physiological stimuli (e.g., atheroprotective flow) and cardiovascular drugs (e.g., statins) exert their beneficial effects in part through the induction of KLF4 in ECs and monocytes[1, 2]. While a higher level of KLF4 in ECs regulates the expression of genes such as endothelial nitric oxide synthase (eNOS)[3, 4], induction of KLF4 in the macrophage favors the transition from the pro-inflammatory M1 to anti-inflammatory M2 phenotype[5]. At the disease level, the atheroprotective role of KLF4 in ECs and monocytes/macrophages is demonstrated by increased atherosclerosis in ApoE-null mice with either EC-specific or myeloid-specific KLF4 ablation[6, 7].

Cholesterol 25-hydroxylase (Ch25h) modulates cholesterol and lipid metabolism by converting cholesterol to 25-hydroxycholesterol (25-HC)[8]. Recent studies demonstrate that 25-HC, the product of Ch25h, increases the anti-viral effect and innate immunity in the host[9–11]. Liu *et al.* indicated that interferon enhances Ch25h-25-HC which suppressed viral growth through blocking virus fusion to the host cell membrane[12]. Reboldi *et al.* found that Ch25h-25-HC suppresses NOD-like receptor family, pyrin domain containing protein 3 (NLRP3) inflammasome-dependent interleukin-1β (IL-1β) production in macrophages and inhibits septic shock in mouse models[13]. Sterol regulatory element binding protein 2 (SREBP2) and liver X receptor (LXR) are two TFs that regulate cholesterol biosynthesis and metabolism reciprocally[14]. SREBP2 is a key mediator of genes involved in cholesterol biosynthesis [e.g., 3-hydroxy-3-methylglutaryl-coenzyme A (HMG-CoA) reductase] and uptake [e.g., low density lipoprotein (LDL) receptor] as well as induces NLRP3 inflammasome in ECs[15]. Belonging to the nuclear receptor superfamily, LXR transactivates genes such as ATP-binding cassette (ABC) transporters, ABCA1 and ABCG1, to promote

reverse cholesterol transport (RCT)[16]. Ligand-dependent LXR activation in ECs is associated with reduced oxidative stress and increased eNOS activity[17]. Furthermore, administration of a synthetic LXR ligand to ApoE$^{-/-}$ or LDLR$^{-/-}$ mice decreased atherosclerosis[18]. By contrast, bone marrow transplantation from LXRα/β$^{-/-}$ mice to ApoE$^{-/-}$ or LDLR$^{-/-}$ recipients resulted in a marked increase of atherosclerotic lesion size[19]. Interestingly, 25-HC inhibits the transcriptional activity of SREBP2[20], while serving as an agonistic ligand for LXR[21].

The initiation, development, and advancement of atherosclerosis involve multiple inflammatory events in the endothelium, circulatory monocytes, and resident macrophages in the arterial wall. The sum of the pro-inflammatory responses counteracting the anti-inflammatory responses in these cell types determines the progression and severity of atherosclerosis. Given the dual role of 25-HC in inhibiting SREBP2 and activating LXR, we postulate that physiological stimuli and cardiovascular therapeutics that induce KLF4 in the endothelium and/or monocytes/macrophages are atheroprotective, in part through the regulation of Ch25h and LXR. Our results demonstrate that KLF4 transactivates Ch25h and LXR in ECs and macrophages *in vitro* and *in vivo*. Furthermore, the KLF4-Ch25h/LXR axis is atheroprotective, indicated by the increased atherosclerosis in Ch25h$^{-/-}$/ApoE$^{-/-}$ mice.

Methods

See online Supplemental Methods section including Supplemental Tables S1–S5.

Library construction and data processing

Total RNA was extracted and purified using mirVana mRNA isolation kit (Thermo Fisher Scientific) according to the manufacturer's instructions. RNA libraries were prepared for sequencing using standard Illumina protocols. Base calling and quality scoring were performed by an updated implementation of Real-Time Analysis (RTA), termed RTA v2, on the NextSeq 500 system. bcl2fastq Conversion Software v1.8.4 was used to demultiplex data and convert BCL files to FASTQ file formats. Sequenced reads were trimmed for adaptor sequence, and masked for low-complexity or low-quality sequence. Reads were then mapped to the hg19 whole genome for KLF4 overexpression data and mm9 for the Ch25h$^{-/-}$ mouse data using tophat v2.0.14[22]. Reads per kilobase of exon per megabase of library size (RPKM) were calculated using cufflinks v2.2.1[23, 24], which assembles transcripts, estimates their abundances, and tests for differential expression and regulation in RNA-seq samples.

The mapping statistics of Ad-KLF4 versus Ad-null RNA-seq data are shown in Figure S1A. Overall, more than 75% of reads were mapped to the genome. To illustrate the general gene expression pattern of ECs with Ad-KLF4 compared to Ad-null, a genome-wide RNA-seq heat map is shown in Figure S1B, the selected genes with at least 3 RPKM were used for hierarchical clustering. Additionally, the volcano plot in Figure S1C indicating the thresholds used for analysis.

Gene expression network projection

Gene expression data using fold change from two biological repeats of HUVECs infected with Ad-null or Ad-KLF4 were projected to a custom sterol metabolism pathway simplified

from Bloch and Kandustch-Russell pathway (http://lipidmaps.org/pathways/vanted.hmtl). Pathway includes key enzymes and metabolites using Mayachemtools (http://myachemtools.org/) to generate a network gml file to be visualized using Vanted[25, 26].

Binding site prediction

The potential KLF4 binding sites on selected human and mouse genes were predicted with the use of the weight matrix-based program MATCH[27] to scan the promoter regions of the indicated genes. The promoter regions were defined as −3000 to 500 from the transcriptional start site of the genes. CpG islands were predicted by WashU EPI Genome Browser. Primers were designed according to ENCODE ChIP data.

Intracellular cholesterol and cholesterol efflux measurements

Intracellular cholesterol level was measured using a cholesterol fluorometric assay kit from Cayman Chemical. Briefly, macrophages cultured in 6-well plates were lysed with 0.5% Triton X-100 and centrifuged at 13,000 rpm at 4°C for 30 min. Supernatants were then used for the cholesterol measurement. The level of intracellular cholesterol was normalized to the protein concentration of the sample. Cholesterol efflux was measured using Cholesterol Efflux assay kit from Abcam. Briefly, cholesterol was fluorescently labeled and incubated with the isolated peritoneal macrophages (PMs) overnight, HDL was used as the cholesterol acceptor. Fluorescence in the supernatant and cell lysates was measured and cholesterol efflux was estimated as the percentage ratio of fluorescence intensity in the supernatant to the sum of supernatant and PM lysates.

Peritoneal macrophage isolation

Mice were injected with 3% thioglycolate three days prior to sacrifice. PMs were isolated from the mouse peritoneal cavity with PBS. Cells were cultured in DMEM containing 10% fetal bovine serum and 1% penicillin-streptomycin.

ApoE$^{-/-}$/Ch25h$^{-/-}$ mouse line and atherosclerosis study

Animal protocols were approved by Institutional Animal Care and Use Committee of Xi'an Jiaotong University (No. XJTULAC2014-208). ApoE$^{-/-}$ and Ch25h$^{-/-}$ animals were crossbred to obtain ApoE$^{-/-}$/Ch25h$^{-/-}$ and their ApoE$^{-/-}$/Ch25h$^{+/+}$ littermates. To create atherosclerosis, 6-week-old male ApoE$^{-/-}$/Ch25h$^{-/-}$ and the ApoE$^{-/-}$/Ch25h$^{+/+}$ mice were fed a high-fat, high-cholesterol diet (HFD) containing 21% fat, and 1.5% cholesterol (D12079B from Research Diet). Twelve weeks after the HFD, the aorta was isolated to assess the extent and distribution of atherosclerotic lesions by Oil Red-O staining. Lesion area was measured with ImageJ and expressed as a percentage of the total area of aorta. Plasma levels of total cholesterol, high-density lipoprotein cholesterol, low-density lipoprotein cholesterol, and triglycerides were determined using a kit from Nanjing Jiancheng Bioengineering Institution.

Statistical analysis

All data are expressed as mean±SEM. Student's t test was used for comparisons between two groups, or ANOVA for comparisons between multiple groups. If $p<0.05$ after ANOVA

analysis, we then used Bonferroni post-hoc to assess the differences between the two indicated groups, with adjusted $p<0.05$ considered to be statistically significant.

Accession numbers

Transcriptome data of KLF4 overexpression in HUVECs (GSE90982); Transcriptome data of PMs isolated from ApoE$^{-/-}$/Ch25h$^{-/-}$ mice (GSE90983).

Results

KLF4 regulates cholesterol metabolic pathways in ECs

Because endothelial homeostasis is manifested by an optimal level of KLF4 in ECs, we performed RNA-sequencing (RNA-seq) to investigate the transcriptional profile of ECs with adenovirus-mediated overexpression of KLF4 (Ad-KLF4) compared to empty vector (Ad-null). Using gene ontology pathway enrichment tools, i.e., Metascape[28], we analyzed the top 300 upregulated genes to infer the modulated biological processes (Figure S2). KLF4 overexpression increased nitric oxide biosynthesis (GO: 0006809), as well as those involved in vascular development and function [e.g., blood vessel morphogenesis (GO: 0048514), circulatory system process (GO: 0003013), and leukocyte migration (GO: 0050900)]. Unexpectedly, KLF4 overexpression also affected response to lipid (GO: 0033993) (Figure 1A). Following this initial analysis, we further assessed the KLF4-mediated genes that are associated with lipid regulation. Exhibited in the heat map in Figures 1B and S3, cholesterol efflux and oxidation genes were upregulated, whereas the cholesterol biosynthesis genes were downregulated. More specifically, LXRα and LXRβ and their targets [e.g., ABCA1, ABCG1, ApoE, and myosin regulatory light chain interacting protein (MYLIP)] were upregulated, while SREBP2 and its targets (e.g., HMG-CoA reductase and squalene epoxidase) were downregulated. In line with the beneficial effects of KLF4, the expression level of genes involved in EC homeostasis [e.g., peroxisome proliferator activated receptor (PPARα), eNOS, and interleukin (IL)-10] increased and that of pro-inflammatory genes [e.g., NLRP3, monocyte chemoattractant protein (MCP)-1] decreased.

25-HC is not only an agonistic ligand of LXR but also suppresses SREBP2 activation. Thus, the coordinated induction of LXR and suppression of SREBP2 in the RNA-sequencing data suggests that KLF4 might increase the level of 25-HC[20, 21]. Indeed, Ch25h, the enzyme that converts cholesterol to 25-HC, involved in the sterol oxidation KEGG pathway (hsa00120) was upregulated by KLF4 (Figure 1B, 1C). Figure 1C further highlights the Ch25h-mediated switch from cholesterol biosynthesis suppression to activation of cholesterol efflux genes in a cholesterol regulation network. Thus, we concentrated on the role of Ch25h in KLF4-dependent EC homeostasis.

KLF4 transactivates Ch25h in ECs

Given the dual role of 25-HC, we postulated that Ch25h is regulated by KLF4 in ECs, which was validated by the increased expression of Ch25h at both the transcriptional and translational levels in ECs overexpressing KLF4 (Figure 2A and 2B). By using lung ECs isolated from mice with endothelial-specific KLF4 overexpression or KLF4 knockout (i.e., EC-KLF4-Tg or EC-KLF4-KO, respectively), we inferred whether KLF4 induces Ch25h in

endothelium *in vivo*. As expected, the Ch25h mRNA level was significantly lower in ECs from EC-KLF4-KO mice when compared to ECs from EC-KLF4-Tg and wild-type controls (Figure 2C and Figure S4).

Next, we used the bioinformatics tool MATCH to identify 4 putative KLF4 binding sites in the *Ch25h* promoter region and gene body (i.e., −913/902, +607/618, +656/667, and +712/723 bp from the TSS) based on the KLF4 consensus sequence outlined in Figure 2D. To implement the *in silico* prediction, we performed chromatin immunoprecipitation (ChIP) assay to examine whether KLF4 can bind to the *Ch25h* gene. As shown in Figure 2E, KLF4 overexpression in human umbilical vein endothelial cells (HUVECs) had increased enrichment of KLF4 binding to the *Ch25h* promoter at the Site 1 upstream from the TSS whereas the 3 putative sites within the gene body, between +607/618, +656/667, and +712/723 bp, had no significant KLF4 binding. We then created a plasmid construct (Ch25h-Luc) containing the upstream region of the *Ch25h* promoter fused to the luciferase reporter. KLF4 overexpression increased luciferase activity in ECs transfected with Ch25h-Luc when compared with cells infected with Ad-null (Figure 2F). Furthermore, deletion of the region between −913 to −902 bp containing the predicted KLF4 binding Site 1 did not induce luciferase activity (Figure 2F), indicating that this region is needed for KLF4 binding and transactivation of *Ch25h*. Because atheroprotective flow is known to increase the expression of KLF4[1, 2], we next investigated whether pulsatile shear stress (PS), which mimics atheroprotective flow *in vitro*, induces Ch25h in ECs, and if so, whether such induction is KLF4-dependent. As shown in Figure 2G and 2H, the level of KLF4 and Ch25h mRNA and the encoded proteins were all increased by PS, compared to atheroprone flow mimicked by oscillatory shear stress (OS). Conversely, KLF4 knockdown using siRNA decreased PS-induced Ch25h (Figure 2I, 2J). In sum, these results suggest that PS-induced Ch25h is dependent on KLF4 transactivation in ECs.

PS transcriptionally induces Ch25h through epigenetic regulation

KLF4 has been suggested to facilitate the recruitment of transcriptional machinery even to genes within compact chromatin[29]. With KLF4 transactivation of Ch25h in the context of atheroprotective flow, we next examined the epigenetic modulations involved in such activation of the *Ch25h* gene. Utilizing WashU EpiGenome Browser (epigenomegateway.wustl.edu/browser), we identified a CpG island located in the *Ch25h* upstream region between −490 and −989 bp (Figure 3A). This online available data suggests that the *Ch25h* promoter/enhancer region resembles a euchromatic state in HUVECs, which is revealed by the enrichment of the histone modifications including H3K27ac, H3K4me1, and H3K4me3, as well as increased binding of RNA polymerase II (Pol II) (Figure 3A). To investigate whether PS modulates the euchromatic status of this regulatory region, we used methylation-specific qPCR (MSP) to detect DNA methylation and histone-ChIP qPCR to identify the levels of histone markers associated with active transcription (i.e., H3K4me3 and H3K27ac) in the upstream region of the *Ch25h* gene. Compared with OS, PS significantly decreased DNA methylation, but enriched H3K4me3 and H3K27ac in the upstream region (Figure 3B–D), indicating that PS rendered an open and active upstream region for the facilitation of the *Ch25h* gene induction. Similar epigenetic modulations were also observed in ECs overexpressing KLF4 (Figure 3E–G).

For *in vivo* validation of flow-induced Ch25h, we isolated intima, which contains the endothelium[30, 31], from the aortic arch (AA) and thoracic aorta (TA) of C57BL/6 mice. The flow pattern in AA and TA are atheroprone and atheroprotective, respectively[32]. As shown in Figure 3H, the expression of Ch25h mRNA was increased in the TA than that of the AA. Consistently, DNA methylation was reduced while H3K4me3 and H3K27ac were enriched in the *Ch25h* promoter in the TA when compared with the AA (Figure 3I–K). Taken together, these data suggest that epigenetic modulations are highly involved in the atheroprotective flow-induced Ch25h via KLF4.

In parallel to atheroprotective flow, vasoprotective drugs (e.g., statins) also induce KLF4[31, 33]. Thus, we postulated that statins may also achieve its pleotropic effects in ECs in part through the increase of Ch25h. Indeed, treating ECs with atorvastatin induced Ch25h transcriptionally and translationally in a KLF4-dependent manner. Such induction was attenuated when KLF4 was knocked down (Figure S5A, S5B). To study the effects of statins *in vivo*, C57BL/6 mice were intraperitoneally (i.p.) injected with 50 mg/kg atorvastatin for 24 hr. The expression of Ch25h in aorta was significantly increased (Figure S5C). The statin-induced Ch25h, like that of PS, also involved the epigenetic changes in the promoter region of the *Ch25h* gene, namely, a decrease in DNA methylation together with an enrichment of active histone marks, H3K4me3 and H3K27ac (Figure S5D–S5F).

KLF4 transactivates LXR

We next investigated whether the KLF4-Ch25h axis activates LXR. As seen in Figure 4A and 4B, KLF4 overexpression increased the transcription and translation of LXRα. Furthermore, LXRα and its downstream targets, ABCA1 and ABCG1, were found to be reduced in ECs from EC-KLF4-KO when compared to ECs from EC-KLF4-Tg and wild-type mice (Figure 4C, 4D, and Figure S4). To identify whether direct activation of LXR using an agonist could rescue the loss of KLF4, we treated lung ECs isolated from EC-KLF4-KO with T0901317. As shown in Figure S6A, T0901317 induced the expression of ABCA1 and ABCG1 to the same level in wild-type and EC-KLF4-KO lung ECs. However, such treatment with LXR agonist reduced the suppression of pro-inflammatory SREBP2 and NLRP3 in EC-KLF4-KO lung ECs (Figure S6A). These data further suggest that KLF4 is upstream of LXRα, thus the LXR agonist can restore the anti-inflammatory phenotype seen when KLF4 is knocked out. To investigate the role of endogenous KLF4 in maintaining EC homeostasis in response to lipids, we treated lung ECs from wild-type and EC-KLF4-KO mice with water soluble cholesterol (i.e., cholesterol-methyl-beta-cyclodextrin). In wild-type lung ECs, cholesterol treatment induced the expression of Ch25h, LXRα, ABCA1, ABCG1 (Figure S6B). Cholesterol, as the substrate for Ch25h, could then be converted to 25-HC promoting LXRα expression and cholesterol efflux to maintain EC homeostasis. Conversely, KLF4-KO ECs had reduced induction of Ch25h, LXRα, and LXR downstream targets with or without cholesterol rich conditions (Figure S6B). Furthermore, when KLF4-KO ECs were treated with cholesterol, NLRP3 was elevated, suggesting that EC homeostasis could not be maintained and the balance was pushed towards a pro-inflammatory phenotype (Figure S6B). Consistently, KLF4 overexpression upregulated LXRα target genes (i.e., ABCA1 and ABCG1) while Ch25h knockdown attenuated the KLF4 induction of ABCA1 and ABCG1 (Figure 4E). With respect to EC inflammatory status, KLF4 overexpression suppressed

SREBP2 and NLRP3 expression, while Ch25h knockdown de-repressed these pro-inflammatory mediators (Figure 4F). As a rescue experiment, we found that NLRP3 inflammasome activity, revealed by IL-18 cleavage, was also suppressed when ECs were treated with 25-HC or T0901317 (Figure S6C). However, using KLF4 overexpression to attempt to rescue LXR in ECs isolated from Ch25h$^{-/-}$ mice resulted in induction of LXR, ABCA1, and ABCG1, while SREBP2 and NLRP3 remained unchanged (Figure S6D). These results are consistent with the siRNA knockdown experiments in Figure 4E and 4F, which suggest the causality among KLF4 and Ch25h. To further evaluate whether the beneficial role of KLF4 is dependent on LXR, we overexpressed KLF4 in ECs and then treated with GSK 2033 (an LXR antagonist). GSK 2033 caused the blockade of ABCA1, ABCG1, eNOS, while elevating NLRP3 (Figure S6E). In sum, these data suggest that KLF4-mediated EC homeostasis is dependent on both Ch25h and LXR.

Using MATCH, we predicted the presence of several putative KLF4 binding sites located in the promoter region of the *LXRα* gene (Figure 4G), suggesting that KLF4 may directly transactivate *LXRα*. Interestingly, according to the WashU EpiGenome Browser, the upstream region of the *LXRα* gene in unstimulated HUVECs is euchromatic and thus would be accessible for KLF4 binding (Figure S7). Using ChIP assays, we demonstrated that KLF4 overexpression resulted in KLF4 enrichment in the *LXRα* promoter (Figure 4H). Further validation using luciferase reporters determined that KLF4 overexpression increased luciferase activity, which indicated KLF4 transactivation of LXRα (Figure 4I). Given that PS transcriptionally upregulates LXRα[34], we next demonstrated that KLF4 knockdown with siRNA attenuated PS-induced LXRα (Figure 4J). For *in vivo* relevance, we found that LXRα, ABCA1, and ABCG1 expression was augmented in TA when compared to AA (Figure 4K). ECs express both LXRα and LXRβ[35]. Noticeably, KLF4 regulated LXRβ in a similar manner as that of LXRα (Figure S7, S8). Collectively, data in Figure 4 and Figures S6–S8 suggest that PS-induced KLF4 upregulates ABCA1 and ABCG1 in ECs, which is dependent on Ch25h and LXR.

KLF4-Ch25h/LXR promotes macrophage polarization

The atheroprotective role of KLF4 is not only due to its effects in ECs, but also in circulating monocytes and resident macrophages in the vessel wall[6, 7]. To examine whether KLF4 regulation of Ch25h and LXR is common in macrophages, we overexpressed KLF4 in a mouse macrophage cell line (i.e., RAW264.7 cells). The expression of Ch25h, LXRα, LXRβ, ABCA1, and ABCG1 were all increased (Figure 5A). Furthermore, LC-MS/MS data suggested that intracellular concentration of 25-HC was increased in cultured THP-1 monocytes overexpressing KLF4 (Figure 5B). Similar to ECs, LXR agonist was able to induce the expression of ABCA1 and ABCG1 in peritoneal macrophages (PMs) isolated from myeloid-specific KLF4-KO (mye-KLF4-KO) mice (Figure S9A). We also examined the role of endogenous KLF4 in macrophages under cholesterol rich conditions by treating PMs isolated from mye-KLF4-KO or wild-type mice with cholesterol. Results shown in Figure S9B demonstrated that KLF4 ablation led to reduced cholesterol efflux and enhanced pro-inflammatory status in PMs. These data suggest that KLF4 may have analogous atheroprotective functions in both ECs and macrophages.

Treating bone marrow-derived macrophages (BMDMs) with 25-HC resulted in a temporal suppression of SREBP2 and its downstream targets in cholesterol biosynthesis as well as increased Ch25h and LXR targets[36]. Further analysis of these mined data demonstrates that 25-HC also decreased the expression of those involved in NLRP3 inflammasome (i.e., NLRP3, ASC, IL-1β and IL-18) and pro-inflammatory M1 pathways [i.e., IL-6, TNFα, Gro1, and cyclooxygenase-2 (COX2)], while increased those anti-inflammatory M2 markers [i.e., mannose receptor, C type 1 (Mrc1), arginase-1 (Arg1)] (Figure 5C). In light of these analyses and because KLF4 overexpression in macrophages leads to the M1-to-M2 transition[5], we investigated the causative effect of Ch25h-25-HC in the KLF4-mediated macrophage polarization. When RAW264.7 cells were treated with 25-HC, we validated that the mRNA expression of pro-inflammatory genes (e.g., NLRP3, IL-1β) and M1 marker genes [i.e., COX2, TNFα, chemokine (C-C motif) ligand 5 (CCL5), inducible nitric oxide synthase (iNOS), and IL-6] were suppressed while those of the M2 marker genes [i.e., peroxisome proliferator-activated receptor γ (PPARγ), Mrc1, chitinase-like 3 (chil3), Arg1, resistin like alpha (retnla), and IL-10] were increased (Figure 5D). In contrast, Ch25h knockdown in RAW264.7 cells increased the expression of the aforementioned pro-inflammatory and M1 marker genes while decreased the mRNA levels of the M2 marker genes when compared with the control siRNA (Figure 5E). Correspondingly, KLF4-mediated M2 markers were inhibited while M1 markers were de-suppressed when macrophages were treated with an LXR antagonist (Figure S10A). To further examine the role of Ch25h in macrophage polarization *in vivo*, we isolated peritoneal macrophages (PMs) from $Ch25h^{-/-}$ mice and their $Ch25h^{+/+}$ littermates. As seen in Figure 5F–5H, reduced expression of LXR and LXR targets, increased expression of SREBP and SREBP downstream, a higher total cholesterol content, and decreased cholesterol efflux were found in $Ch25h^{-/-}$ macrophages, when compared with those in $Ch25h^{+/+}$ littermates. Furthermore, KLF4 overexpression in $Ch25h^{-/-}$ macrophages resulted in incremental induction of LXR and LXR downstream targets (Figure S10B), similar to the rescue experiment performed in $Ch25h^{-/-}$ ECs (Figure S6D). In addition, $Ch25h^{-/-}$ macrophages showed increased levels of inflammatory and M1 markers while suppressing M2 markers (Figure 5I). As a rescue experiment, $Ch25h^{-/-}$ macrophages co-incubated with 25-HC exhibited decreased expression of inflammatory and M1 markers while increasing the expression of M2 markers (Figure 5J). Collectively, Figures 5, S9, and S10 demonstrated that KLF4 substantially induced Ch25h and LXR in macrophages, similar to that in ECs. Functionally, such induction promoted M2 polarization and regulated cholesterol content in part through augmented RCT.

Ch25h ablation increases atherosclerosis susceptibility

Because the involvement of Ch25h-25-HC in functional endothelium and anti-inflammatory phenotype in macrophages, we utilized $Ch25h^{-/-}$ mice to investigate the comprehensive role of Ch25h in atherosclerosis. We introduced $ApoE^{-/-}$ background into $Ch25h^{-/-}$ mice to promote atherosclerotic lesion development. RNA-seq was performed to confirm the pro-inflammatory status and M2 to M1 phenotype in PMs isolated from the $ApoE^{-/-}/Ch25h^{-/-}$ mice. As shown in Figure 6A and S11, while Ch25h and LXRα were decreased, the pro-inflammatory CCL5, iNOS, IL-1β, were increased in these PMs. Feeding 12 weeks of an atherogenic diet, there was no significant difference in body weight, serum triglyceride,

cholesterol, LDL and HDL between ApoE$^{-/-}$/Ch25h$^{-/-}$ and their ApoE$^{-/-}$/Ch25h$^{+/+}$ littermates (Table S6). The mean lesion area in the aortic root, where the blood flow pattern is most disturbed[30], was ~1.9-fold larger for ApoE$^{-/-}$/Ch25h$^{-/-}$ mice than ApoE$^{-/-}$/Ch25h$^{+/+}$ littermates (89.7 ± 36.1 μm^{2}x10^3 vs. 45.0 ± 32.3 μm^{2}x10^3, respectively) (Figure 6B). Additionally, H&E staining revealed increased cell density which was largely composed of infiltrating macrophages demonstrated by MAC1 staining as well as decreased CD31 staining (Figure 6B). *En face* Oil Red-O staining revealed that the mean lesion area in the thoracic aorta and that of aortic arch was also augmented for ApoE$^{-/-}$/Ch25h$^{-/-}$ than ApoE$^{-/-}$/Ch25h$^{+/+}$ mice (19.5 ± 8.5% vs. 10.1 ± 4.1% and 44.1 ± 9.0% vs. 29.7 ± 9.6%, respectively) (Figure 6C). The total lesion area as the sum of aortic arch, thoracic aorta, and abdominal aorta remained greater for ApoE$^{-/-}$/Ch25h$^{-/-}$ when compared to the ApoE$^{-/-}$/Ch25h$^{+/+}$ littermates (24.5 ± 7.3% vs. 13.9 ± 5.0%) (Figure 6C). Thus, the systemic ablation of Ch25h plays a critical role in accelerated atherosclerosis.

Discussion

The current study encompassing research on both ECs and macrophages provides experimental evidence of the atheroprotective role of KLF4 via the induction of Ch25h and LXR. Initially, RNA-seq data revealed that KLF4, through transactivating Ch25h and LXR, is a novel mediator of cholesterol homeostasis in ECs in addition to its canonical role in nitric oxide biosynthesis, blood vessel, and circulatory system processes[37,38]. Microarray data from 25-HC-treated BMDMs (Figure 5C) and from PMs isolated from the ApoE$^{-/-}$/Ch25h$^{-/-}$ mice (Figure 6A) indicated that 25-HC, the catalytic product of Ch25h, was essential to preserve the M2 macrophage polarization. Because Ch25h and LXR are critically involved in the cross-talk between the immune system and cholesterol metabolism[39], KLF4 plays an important role in maintaining vascular homeostasis through its regulation of Ch25h and LXR. The implication of this finding at the disease level is that increased atherosclerosis susceptibility is a common phenotype between ApoE$^{-/-}$/Ch25h$^{-/-}$ (Figure 6) and ApoE$^{-/-}$ mice with KLF4 or LXR ablation in the endothelium or macrophages[16,19,40]. Given atherosclerosis is a multifaceted vascular impairment composed of several cell types including ECs and macrophages[41], the atheroprone phenotype among these mouse lines suggests that the KLF4-Ch25h/LXR axis in ECs and macrophages acts synergistically, which is atheroprotective *in vivo*.

Serving as a ligand to LXR while inhibiting SREBP2 activation, 25-HC maintains a balance between cholesterol efflux and cholesterol biosynthesis[11]. Cholesterol efflux, regulated by LXR downstream targets such as ABCA1 and ABCG1, is known to be mediated by the innate immune response in macrophages[42]. Furthermore, upregulated SREBP is associated with unresolved innate immunity, leading to inflammasome activation in both ECs and macrophages[15,43]. Here, we further defined that KLF4 regulates a counterbalance between LXR and SREBP via the regulation of Ch25h-25-HC. Although, endogenous KLF4 may be supplemental in mitigating LXR responses as target gene expression remains intact even with the loss of KLF4 (Figure S6A and S9A). In addition to the beneficial role in regulating LXR and SREBP, 25-HC exerts anti-viral effects through inhibiting viral particle uptake[11] and activates integrated stress response (ISR) genes to reprogram transcription and translation[35]. However, the anti-inflammatory role of 25-HC remains somewhat

controversial as others have indicated that the oxysterol promotes macrophage foam cell formation and is increased in atherosclerotic lesions[44]. Such contradiction may be due, in part, to the differences in experimental conditions and requires further investigation.

Endothelial and macrophage homeostasis relies on an optimal level of KLF4, which can be induced by both physiological and pharmacological stimuli such as shear stress and statins[44]. At the tissue level, KLF4 overexpression in the endothelium is atheroprotective[6]. Due to sequence homology between KLF4 and KLF2 and because both are well-known in atheroprotection[45,46], we also examined the role of KLF2 in Ch25h expression. As shown in Figure S12, KLF2 increased Ch25h mRNA and protein expression. In light of statin-induced KLF2 and KLF4 in ECs[45], we also found that statin treatment of ECs increased Ch25h in a KLF4-dependent manner (Figure S5). If statin can activate KLF4 in the endothelium *in vivo*, the consequent induction of Ch25h and LXR would be one of the pleotropic effects of statin therapy. KLF4 also mediates macrophage polarization as KLF4 is drastically induced in M2 macrophages but significantly reduced in M1 macrophages[5]. Phenotypically, mice with myeloid KLF4 deficiency are characterized by increased bactericidal activity and delayed wound healing, signifying M1 polarization[5]. Collectively, our data support that Ch25h-25-HC play a major role in the vascular beneficial effects caused by physiological and pharmacological stimuli (e.g., PS and statins) that activate KLF4.

Regarding stimuli which downregulate KLF4 in the vasculature, we and others have previously shown that oxidative and inflammatory burdens, exemplified by oxLDL, angiotensin II, and hydrogen peroxide, activate the SREBP2-miR-92a axis, which in turn suppresses KLF4 in ECs[47]. Thus, under atherogenic conditions, the KLF4 level is likely to be reduced in both the endothelium and macrophages via SREBP2-miR-92a. Noticeably, KLF4 overexpression not only increased the level of Ch25h and LXR, but also reduced SREBP2 and miR-33 (Figure S13). Given miR-33 targets ABCA1 and ABCG1[48], aberrant KLF4 expression may feed forward to further downregulate RCT. Furthermore, single and double ablation of mouse *abca1* and *abcg1* specifically in the endothelium are pro-atherogenic, not only through the reduction in RCT but also through the perturbation of eNOS[49]. In conjunction with the current study, the suggested mechanisms constitute a regulatory network linking endothelial dysfunction and macrophage polarization, which aggravates atherosclerosis (see Figure 7).

KLF4 has been suggested to be a “pioneer transcription factor” along with OCT4, c-MYC, and SOX2[29]. Pioneer transcription factors are able to directly bind to DNA and modify nucleosome complexes allowing the chromatin structure to relax[50]. We found that KLF4 transactivation of *Ch25h*, *LXRα*, and *LXRβ* involves direct *cis*-element binding measured through ChIP assays (Figures 2E, 4H, and S8D). Furthermore, KLF4 can function as a transcriptional repressor of SREBP2[51]. Therefore, we performed ChIP assays for key cholesterol efflux/oxidation and cholesterol biosynthesis genes to define a range of KLF4 direct interactions. Further analysis demonstrated that KLF4 can directly bind to ABCA1, ABCG1, and ApoE to promote expression, while also binding to SREBP2 and MVK to suppress transcription (Figure S14). Thus, beneficial stimuli which enhance KLF4 expression, such as atheroprotective flow and statins, would increase KLF4 interaction with the cognate DNA binding sequences. Further chromatin relaxation is likely through the

trans-dependent modifications of H3K27ac and H3K4me3 as shown in Figure 3. Additionally, both atheroprotective flow and KLF4 overexpression reduced DNA methylation in the promoter region of *Ch25h*. However, promoter methylation of several atheroprotective genes was increased by atheroprone flow, resulting from increased expression of DNA methyltransferase 1 (DNMT1) and DNMT3a[52,53]. KLF4 is able to directly bind to methylated DNA, of which the function remains elusive but has been eluded to be required for cellular reprogramming and stem cell differentiation[54,55]. As a pioneering transcription factor, whether KLF4 regulates the epigenetic landscape of an array of genes crucial for EC function at the genome-wide scale warrants further study.

In summary, this study identifies that KLF4 is a mediator for both Ch25h and LXR in ECs and macrophages. As atherogenesis includes dysfunctional endothelium as well as M1 polarized macrophages with attendant decrease of KLF4, we suggest that the congruent KLF4-Ch25h/LXR axis in both cell types is anti-atherogenic.

Supplementary Material

Refer to Web version on PubMed Central for supplementary material.

Acknowledgments

The authors would like to thank Dr. Christopher K. Glass at the University of California, San Diego for his thoughtful suggests. Also, Dr. Yue Han at the University of California, San Diego, and Mr. Baochang Lai, Ms. Yaqiong Wang, and Yanjun Yin at the Xi'an Jiaotong University, Xi'an, China, for their assitance with experiments, and Dr. Nanping Wang at the Xi'an Jiaotong University, Xi'an, China, for the KLF4 adenovirus.

Sources of Funding

This work was supported by the National Institutes of Health grants R01HL105318 and R01HL1125643 (J.Y.S.), 5T32HL007444 (M. Martin), 1R01ES027595-01 and 1S10OD020025-01 (M.J. and Y.X.); the National Natural Science Foundation of China 81270349 and 81670452 (J.Y.S.); and Xi'an Jiaotong University Financial support.

References

1. Ohnesorge N, Viemann D, Schmidt N, Czymai T, Spiering D, Schmolke M, Ludwig S, Roth J, Goebeler M, Schmidt M. Erk5 activation elicits a vasoprotective endothelial phenotype via induction of Kruppel-like factor 4 (KLF4). J Biol Chem. 2010; 285:26199–26210. [PubMed: 20551324]
2. Clark PR, Jensen TJ, Kluger MS, Morelock M, Hanidu A, Qi Z, Tatake RJ, Pober JS. MEK5 is activated by shear stress, activates ERK5 and induces KLF4 to modulate TNF responses in human dermal microvascular endothelial cells. Microcirculation. 2011; 18:102–117. [PubMed: 21166929]
3. Shen B, Smith RS Jr, Hsu YT, Chao L, Chao J. Kruppel-like factor 4 is a novel mediator of Kallistatin in inhibiting endothelial inflammation via increased endothelial nitric-oxide synthase expression. J Biol Chem. 2009; 284:35471–35478. [PubMed: 19858207]
4. Chiplunkar AR, Curtis BC, Eades GL, Kane MS, Fox SJ, Haar JL, Lloyd JA. The Kruppel-like factor 2 and Kruppel-like factor 4 genes interact to maintain endothelial integrity in mouse embryonic vasculogenesis. BMC Dev Biol. 2013; 13:40. [PubMed: 24261709]
5. Liao X, Sharma N, Kapadia F, Zhou G, Lu Y, Hong H, Paruchuri K, Mahabeleshwar GH, Dalmas E, Venteclef N, Flask CA, Kim J, Doreian BW, Lu KQ, Kaestner KH, Hamik A, Clement K, Jain MK. Kruppel-like factor 4 regulates macrophage polarization. J Clin Invest. 2011; 121:2736–2749. [PubMed: 21670502]
6. Zhou G, Hamik A, Nayak L, Tian H, Shi H, Lu Y, Sharma N, Liao X, Hale A, Boerboom L, Feaver RE, Gao H, Desai A, Schmaier A, Gerson SL, Wang Y, Atkins GB, Blackman BR, Simon DI, Jain

MK. Endothelial Kruppel-like factor 4 protects against atherothrombosis in mice. J Clin Invest. 2012; 122:4727–4731. [PubMed: 23160196]

7. Sharma N, Lu Y, Zhou G, Liao X, Kapil P, Anand P, Mahabeleshwar GH, Stamler JS, Jain MK. Myeloid KLF4 deficiency augments atherogenesis in ApoE−/− mice. Arterioscler Thromb Vasc Biol. 2012; 32:2836–2838. [PubMed: 23065827]
8. Tuong ZK, Lau P, Du X, Condon ND, Goode JM, Oh TG, Yeo JC, Muscat GE, Stow JL. RORalpha and 25-Hydroxycholesterol Crosstalk Regulates Lipid Droplet Homeostasis in Macrophages. PLoS One. 2016; 11:e0147179. [PubMed: 26812621]
9. Bauman DR, Bitmansour AD, McDonald JG, Thompson BM, Liang G, Russell DW. 25-Hydroxycholesterol secreted by macrophages in response to Toll-like receptor activation suppresses immunoglobulin A production. Proc Natl Acad Sci U S A. 2009; 106:16764–16769. [PubMed: 19805370]
10. Blanc M, Hsieh WY, Robertson KA, Kropp KA, Forster T, Shui G, Lacaze P, Watterson S, Griffiths SJ, Spann NJ, Meljon A, Talbot S, Krishnan K, Covey DF, Wenk MR, Craigon M, Ruzsics Z, Haas J, Angulo A, Griffiths WJ, Glass CK, Wang Y, Ghazal P. The transcription factor STAT-1 couples macrophage synthesis of 25-hydroxycholesterol to the interferon antiviral response. Immunity. 2013; 38:106–118. [PubMed: 23273843]
11. Cyster JG, Dang EV, Reboldi A, Yi T. 25-Hydroxycholesterols in innate and adaptive immunity. Nat Rev Immunol. 2014; 14:731–743. [PubMed: 25324126]
12. Liu SY, Aliyari R, Chikere K, Li G, Marsden MD, Smith JK, Pernet O, Guo H, Nusbaum R, Zack JA, Freiberg AN, Su L, Lee B, Cheng G. Interferon-inducible cholesterol-25-hydroxylase broadly inhibits viral entry by production of 25-hydroxycholesterol. Immunity. 2013; 38:92–105. [PubMed: 23273844]
13. Reboldi A, Dang EV, McDonald JG, Liang G, Russell DW, Cyster JG. Inflammation. 25-Hydroxycholesterol suppresses interleukin-1-driven inflammation downstream of type I interferon. Science. 2014; 345:679–684. [PubMed: 25104388]
14. Dushkin MI. Macrophage/foam cell is an attribute of inflammation: mechanisms of formation and functional role. Biochemistry (Mosc). 2012; 77:327–338. [PubMed: 22809150]
15. Xiao H, Lu M, Lin TY, Chen Z, Chen G, Wang WC, Marin T, Shentu TP, Wen L, Gongol B, Sun W, Liang X, Chen J, Huang HD, Pedra JH, Johnson DA, Shyy JY. Sterol regulatory element binding protein 2 activation of NLRP3 inflammasome in endothelium mediates hemodynamic-induced atherosclerosis susceptibility. Circulation. 2013; 128:632–642. [PubMed: 23838163]
16. Schuster GU. Accumulation of Foam Cells in Liver X Receptor-Deficient Mice. Circulation. 2002; 106:1147–1153. [PubMed: 12196343]
17. Hayashi T, Kotani H, Yamaguchi T, Taguchi K, Iida M, Ina K, Maeda M, Kuzuya M, Hattori Y, Ignarro LJ. Endothelial cellular senescence is inhibited by liver X receptor activation with an additional mechanism for its atheroprotection in diabetes. Proc Natl Acad Sci U S A. 2014; 111:1168–1173. [PubMed: 24398515]
18. Joseph SB, McKilligin E, Pei L, Watson MA, Collins AR, Laffitte BA, Chen M, Noh G, Goodman J, Hagger GN, Tran J, Tippin TK, Wang X, Lusis AJ, Hsueh WA, Law RE, Collins JL, Willson TM, Tontonoz P. Synthetic LXR ligand inhibits the development of atherosclerosis in mice. Proc Natl Acad Sci U S A. 2002; 99:7604–7609. [PubMed: 12032330]
19. Tangirala RK, Bischoff ED, Joseph SB, Wagner BL, Walczak R, Laffitte BA, Daige CL, Thomas D, Heyman RA, Mangelsdorf DJ, Wang X, Lusis AJ, Tontonoz P, Schulman IG. Identification of macrophage liver X receptors as inhibitors of atherosclerosis. Proc Natl Acad Sci U S A. 2002; 99:11896–11901. [PubMed: 12193651]
20. Adams CM, Reitz J, De Brabander JK, Feramisco JD, Li L, Brown MS, Goldstein JL. Cholesterol and 25-hydroxycholesterol inhibit activation of SREBPs by different mechanisms, both involving SCAP and Insigs. J Biol Chem. 2004; 279:52772–52780. [PubMed: 15452130]
21. Lehmann JM, Kliewer SA, Moore LB, Smith-Oliver TA, Oliver BB, Su JL, Sundseth SS, Winegar DA, Blanchard DE, Spencer TA, Willson TM. Activation of the nuclear receptor LXR by oxysterols defines a new hormone response pathway. J Biol Chem. 1997; 272:3137–3140. [PubMed: 9013544]

22. Kim D, Pertea G, Trapnell C, Pimentel H, Kelley R, Salzberg SL. TopHat2: accurate alignment of transcriptomes in the presence of insertions, deletions and gene fusions. Genome Biol. 2013; 14:R36. [PubMed: 23618408]

23. Roberts A, Trapnell C, Donaghey J, Rinn JL, Pachter L. Improving RNA-Seq expression estimates by correcting for fragment bias. Genome Biol. 2011; 12:R22. [PubMed: 21410973]

24. Trapnell C, Williams BA, Pertea G, Mortazavi A, Kwan G, van Baren MJ, Salzberg SL, Wold BJ, Pachter L. Transcript assembly and quantification by RNA-Seq reveals unannotated transcripts and isoform switching during cell differentiation. Nature Biotechnol. 2010; 28:511–515. [PubMed: 20436464]

25. Rohn H, Junker A, Hartmann A, Grafahrend-Belau E, Treutler H, Klapperstuck M, Czauderna T, Klukas C, Schreiber F. VANTED v2: a framework for systems biology applications. BMC Syst Biol. 2012; 6:139. [PubMed: 23140568]

26. Maurya MR, Gupta S, Li X, Fahy E, Dinasarapu AR, Sud M, Brown HA, Glass CK, Murphy RC, Russell DW, Dennis EA, Subramaniam S. Analysis of inflammatory and lipid metabolic networks across RAW264.7 and thioglycolate-elicited macrophages. J Lipid Res. 2013; 54:2525–2542. [PubMed: 23776196]

27. Kel AE, Gossling E, Reuter I, Cheremushkin E, Kel-Margoulis OV, Wingender E. MATCH: A tool for searching transcription factor binding sites in DNA sequences. Nucleic Acids Res. 2003; 31:3576–3579. [PubMed: 12824369]

28. Tripathi S, Pohl MO, Zhou Y, Rodriguez-Frandsen A, Wang G, Stein DA, Moulton HM, DeJesus P, Che J, Mulder LC, Yanguez E, Andenmatten D, Pache L, Manicassamy B, Albrecht RA, Gonzalez MG, Nguyen Q, Brass A, Elledge S, White M, Shapira S, Hacohen N, Karlas A, Meyer TF, Shales M, Gatorano A, Johnson JR, Jang G, Johnson T, Verschueren E, Sanders D, Krogan N, Shaw M, Konig R, Stertz S, Garcia-Sastre A, Chanda SK. Meta- and Orthogonal Integration of Influenza "OMICs" Data Defines a Role for UBR4 in Virus Budding. Cell host & microbe. 2015; 18:723–735. [PubMed: 26651948]

29. Soufi A, Garcia MF, Jaroszewicz A, Osman N, Pellegrini M, Zaret KS. Pioneer transcription factors target partial DNA motifs on nucleosomes to initiate reprogramming. Cell. 2015; 161:555–568. [PubMed: 25892221]

30. Assemat P, Armitage JA, Siu KK, Contreras KG, Dart AM, Chin-Dusting JP, Hourigan K. Three-dimensional numerical simulation of blood flow in mouse aortic arch around atherosclerotic plaques. Appl Math Model. 2014; 38:4175–4185.

31. Yoshida T, Yamashita M, Iwai M, Hayashi M. Endothelial Kruppel-Like Factor 4 Mediates the Protective Effect of Statins against Ischemic AKI. J Am Soc Nephrol. 2016; 27:1379–1388. [PubMed: 26471129]

32. Chiu JJ, Chien S. Effects of Disturbed Flow on Vascular Endothelium: Pathophysiological Basis and Clinical Perspectives. Physiol Rev. 2011; 91(1):327–387. [PubMed: 21248169]

33. Maejima T, Inoue T, Kanki Y, Kohro T, Li G, Ohta Y, Kimura H, Kobayashi M, Taguchi A, Tsutsumi S, Iwanari H, Yamamoto S, Aruga H, Dong S, Stevens JF, Poh HM, Yamamoto K, Kawamura T, Mimura I, Suehiro J, Sugiyama A, Kaneki K, Shibata H, Yoshinaka Y, Doi T, Asanuma A, Tanabe S, Tanaka T, Minami T, Hamakubo T, Sakai J, Nozaki N, Aburatani H, Nangaku M, Ruan X, Tanabe H, Ruan Y, Ihara S, Endo A, Kodama T, Wada Y. Direct evidence for pitavastatin induced chromatin structure change in the KLF4 gene in endothelial cells. PLoS One. 2014; 9:e96005. [PubMed: 24797675]

34. Zhu M, Fu Y, Hou Y, Wang N, Guan Y, Tang C, Shyy JY, Zhu Y. Laminar shear stress regulates liver X receptor in vascular endothelial cells. Arterioscler Thromb Vasc Biol. 2008; 28:527–533. [PubMed: 18096827]

35. Calkin AC, Tontonoz P. Liver x receptor signaling pathways and atherosclerosis. Arterioscler Thromb Vasc Biol. 2010; 30:1513–1518. [PubMed: 20631351]

36. Shibata N, Carlin AF, Spann NJ, Saijo K, Morello CS, McDonald JG, Romanoski CE, Maurya MR, Kaikkonen MU, Lam MT, Crotti A, Reichart D, Fox JN, Quehenberger O, Raetz CRH, Sullards MC, Murphy RC, Merrill AH, Brown HA, Dennis EA, Fahy E, Subramaniam S, Cavener DR, Spector DH, Russell DW, Glass CK. 25-Hydroxycholesterol Activates the Integrated Stress Response to Reprogram Transcription and Translation in Macrophages. J Biol Chem. 2013; 288:35812–35823. [PubMed: 24189069]

37. Kunes P, Holubcova Z, Krejsek J. Occurrence and significance of the nuclear transcription factor Kruppel-like factor 4 (KLF4) in the vessel wall. Acta medica (Iran). 2009; 52:135–139.
38. Yoshida T, Hayashi M. Role of Kruppel-like factor 4 and its binding proteins in vascular disease. J Atheroscler Thromb. 2014; 21:402–413. [PubMed: 24573018]
39. Simon A. Cholesterol metabolism and immunity. N Engl J Med. 2014; 371:1933–1935. [PubMed: 25390746]
40. Bradley MN, Hong C, Chen M, Joseph SB, Wilpitz DC, Wang X, Lusis AJ, Collins A, Hseuh WA, Collins JL, Tangirala RK, Tontonoz P. Ligand activation of LXR beta reverses atherosclerosis and cellular cholesterol overload in mice lacking LXR alpha and apoE. J Clin Invest. 2007; 117:2337–2346. [PubMed: 17657314]
41. Glass CK, Witztum JL. Atherosclerosis. the road ahead. Cell. 2001; 104:503–516. [PubMed: 11239408]
42. Tall AR, Yvan-Charvet L. Cholesterol, inflammation and innate immunity. Nat Rev Immunol. 2015; 15:104–116. [PubMed: 25614320]
43. Im SS, Yousef L, Blaschitz C, Liu JZ, Edwards RA, Young SG, Raffatellu M, Osborne TF. Linking lipid metabolism to the innate immune response in macrophages through sterol regulatory element binding protein-1a. Cell Metab. 2011; 13:540–549. [PubMed: 21531336]
44. Gold ES, Ramsey SA, Sartain MJ, Selinummi J, Podolsky I, Rodriguez DJ, Moritz RL, Aderem A. ATF3 protects against atherosclerosis by suppressing 25-hydroxycholesterol-induced lipid body formation. J Exp Med. 2012; 209:807–817. [PubMed: 22473958]
45. Villarreal G Jr, Zhang Y, Larman HB, Gracia-Sancho J, Koo A, Garcia-Cardena G. Defining the regulation of KLF4 expression and its downstream transcriptional targets in vascular endothelial cells. Biochem Biophys Res Commun. 2010; 391:984–989. [PubMed: 19968965]
46. Basu P, Sargent TG, Redmond LC, Aisenberg JC, Kransdorf EP, Wang SZ, Ginder GD, Lloyd JA. Evolutionary conservation of KLF transcription factors and functional conservation of human gamma-globin gene regulation in chicken. Genomics. 2004; 84:311–319. [PubMed: 15233995]
47. Chen Z, Wen L, Martin M, Hsu CY, Fang L, Lin FM, Lin TY, Geary MJ, Geary GG, Zhao Y, Johnson DA, Chen JW, Lin SJ, Chien S, Huang HD, Miller YI, Huang PH, Shyy JY. Oxidative stress activates endothelial innate immunity via sterol regulatory element binding protein 2 (SREBP2) transactivation of microRNA-92a. Circulation. 2015; 131:805–814. [PubMed: 25550450]
48. Rayner KJ, Suarez Y, Davalos A, Parathath S, Fitzgerald ML, Tamehiro N, Fisher EA, Moore KJ, Fernandez-Hernando C. MiR-33 contributes to the regulation of cholesterol homeostasis. Science. 2010; 328:1570–1573. [PubMed: 20466885]
49. Westerterp M, Tsuchiya K, Tattersall IW, Fotakis P, Bochem AE, Molusky MM, Ntonga V, Abramowicz S, Parks JS, Welch CL, Kitajewski J, Accili D, Tall AR. Deficiency of ATP-binding cassette transporters A1 and G1 in endothelial cells accelerates atherosclerosis in mice. Arterioscler Thromb Vasc Biol. 2016; 36(7):1328–1337. [PubMed: 27199450]
50. Chen T, Dent SY. Chromatin modifiers and remodellers: regulators of cellular differentiation. Nat Rev Genet. 2014; 15:93–106. [PubMed: 24366184]
51. Rowland BD, Bernards R, Peeper DS. The KLF4 tumour suppressor is a transcriptional repressor of p53 that acts as a context-dependent oncogene. Nat Cell Biol. 2005; 7(11):1074–1082. [PubMed: 16244670]
52. Jiang YZ, Jimenez JM, Ou K, McCormick ME, Zhang LD, Davies PF. Hemodynamic disturbed flow induces differential DNA methylation of endothelial Kruppel-Like Factor 4 promoter in vitro and in vivo. Circ Res. 2014; 115:32–43. [PubMed: 24755985]
53. Dunn J, Qiu H, Kim S, Jjingo D, Hoffman R, Kim CW, Jang I, Son DJ, Kim D, Pan C, Fan Y, Jordan IK, Jo H. Flow-dependent epigenetic DNA methylation regulates endothelial gene expression and atherosclerosis. J Clin Invest. 2014; 124:3187–3199. [PubMed: 24865430]
54. Spruijt CG, Gnerlich F, Smits AH, Pfaffeneder T, Jansen PW, Bauer C, Munzel M, Wagner M, Muller M, Khan F, Eberl HC, Mensinga A, Brinkman AB, Lephikov K, Muller U, Walter J, Boelens R, van Ingen H, Leonhardt H, Carell T, Vermeulen M. Dynamic readers for 5-(hydroxy)methylcytosine and its oxidized derivatives. Cell. 2013; 152:1146–1159. [PubMed: 23434322]

55. Hu S, Wan J, Su Y, Song Q, Zeng Y, Nguyen HN, Shin J, Cox E, Rho HS, Woodard C, Xia S, Liu S, Lyu H, Ming GL, Wade H, Song H, Qian J, Zhu H. DNA methylation presents distinct binding sites for human transcription factors. eLife. 2013; 2:e00726. [PubMed: 24015356]

Clinical Perspective

What Is New?

- Krüppel-like factor 4 (KLF4), a key anti-inflammatory transcription factor, up-regulates cholesterol-25-hydroxylase (Ch25h) and liver X receptor (LXR) in vascular endothelial cells (ECs) and macrophages.
- This mechanism enhances reverse cholesterol transport from the vascular wall as well as mitigates inflammation through suppressing sterol regulatory-binding protein 2 (SREBP2) and NOD-like receptor family, pyrin domain containing protein 3 (NLRP3) inflammasome in ECs.
- KLF4-mediated transactivation of Ch25h and LXR also promotes cholesterol efflux and M1 to M2 transition in macrophages.

What Are the Clinical Implications?

- Atherosclerosis is characterized by accumulation of lipids, including cholesterol, in the vascular wall with concurrent increase in vascular inflammation.
- The synergism between the anti-inflammatory effects in both ECs and macrophages contributes to the atheroprotective phenotype.
- Because KLF4 is commonly induced by atheroprotective flow and statins, our results suggest that KLF4 up-regulation of Ch25h and LXR in ECs and macrophages may be a therapeutic target of cardiovascular diseases.

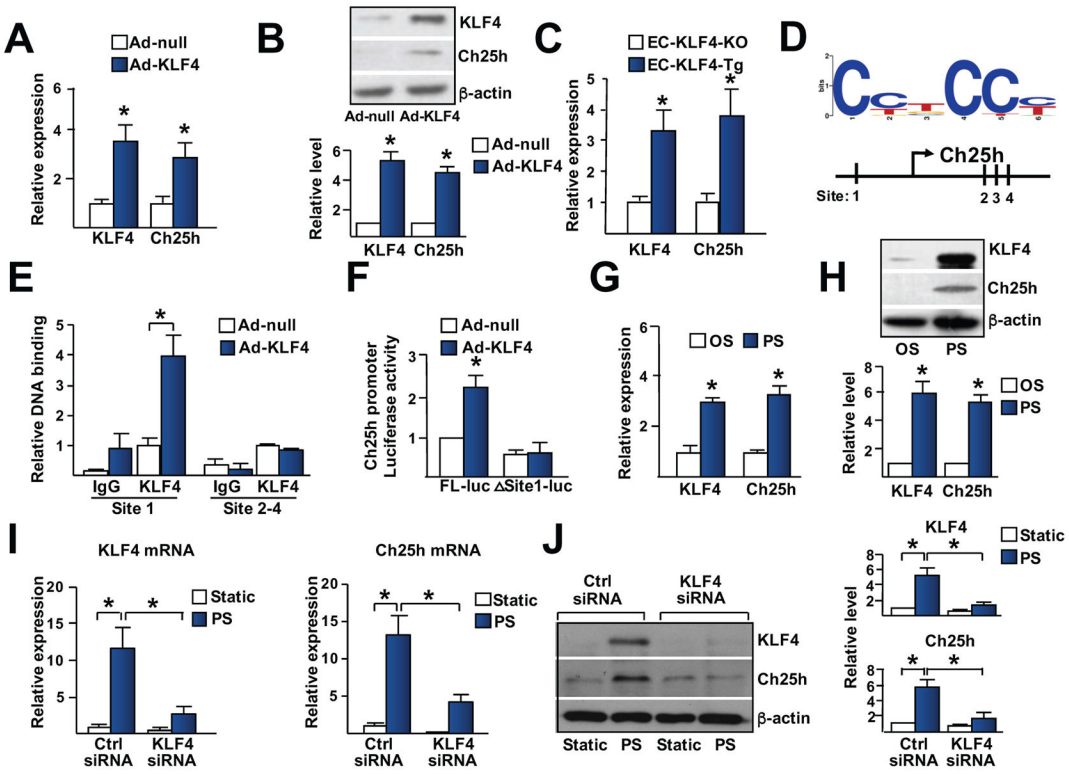

Figure 1. KLF4 regulates cholesterol metabolism in ECs

(A–C) HUVECs were infected with Ad-KLF4 or Ad-null for 48 hr prior to RNA isolation followed by RNA-seq analysis. Data presented are results from two biological repeats (Ad-KLF4 divided by Ad-null). (A) Gene ontology (GO) enrichment using Metascape of the top 300 upregulated genes plotted as −log(p-value). (B) Heat map comparison of Ad-null versus Ad-KLF4 using log2 fold changes of the indicated genes (refer to Figure S3 for heat map of scaled Z-score). (C) Network projection of customized sterol metabolism pathway.

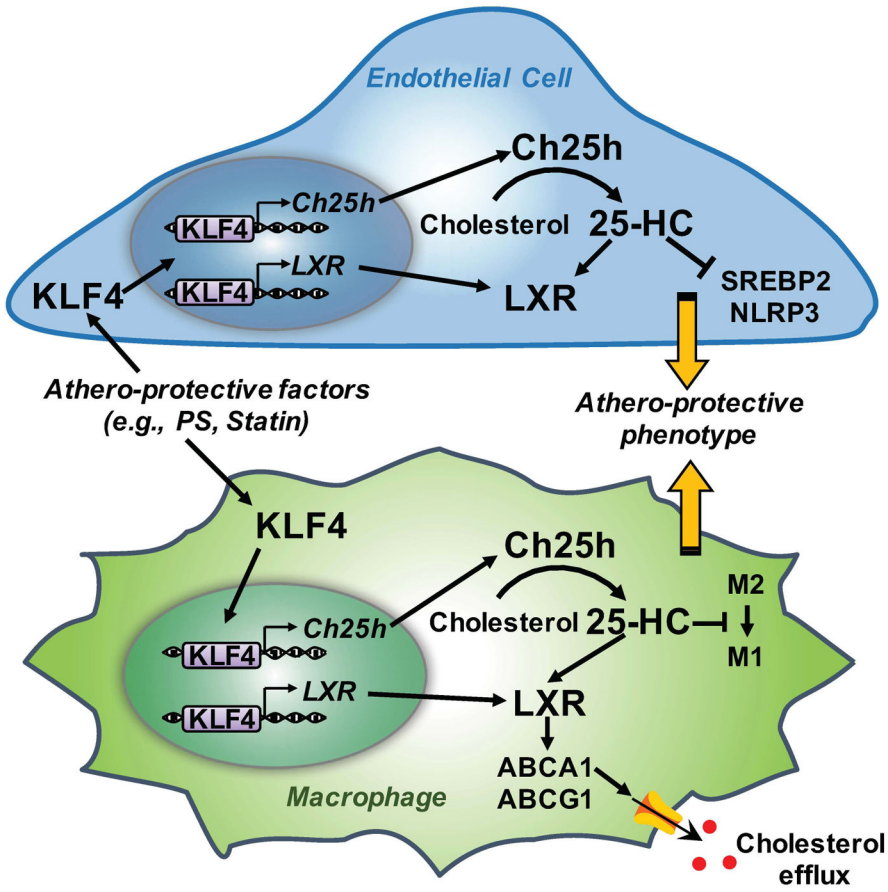

Figure 2. KLF4 transactivates Ch25h in ECs

(A, B) HUVECs were infected with Ad-KLF4 or Ad-null for 24 hr. Expression levels of KLF4 and Ch25h mRNA and protein were measured by qPCR and Western blot, respectively. **(C)** Lung ECs were isolated from EC-specific KLF4 knockout (EC-KLF4-KO) or EC-specific overexpression of KLF4 (EC-KLF4-Tg) mice (n=3 per group). Levels of KLF4 and Ch25h mRNA were measured by qPCR. **(D)** Depiction of the predicted KLF4 binding sites at −913 to −902 bp (Site 1), 607 to 618 bp (Site 2), 656 to 667 bp (Site 3) and 712 to 723 bp (Site 4) in the human *Ch25h* gene. (**E)** HUVECs infected with Ad-KLF4 or Ad-null were analyzed by ChIP assay with the use of anti-KLF4. KLF4 promoter enrichment was quantified by qPCR. IgG was used as an isotype control. **(F)** Bovine aortic endothelial cells (BAECs) were transfected a luciferase reporter fused with the *Ch25h* promoter region (Ch25h-Luc) or with a Site 1 deletion (Ch25hΔS1-Luc) together with pRSV-β-gal reporter for 6 hr, followed by infection with Ad-KLF4 for an additional 24 hr. Luciferase activity was measured and normalized to that of β-gal. **(G, H)** HUVECs were subjected to OS (1±4 dyn/cm^2) or PS (12±4 dyn/cm^2) for 24 hr. **(I, J)** HUVECs were transfected with control siRNA or KLF4 siRNA prior to PS stimulation or kept as a static control for 24 hr. KLF4 and Ch25h mRNA and protein expression were measured by qPCR (G, I) and Western blot (H, J), respectively. Error bars represent mean±SEM from three independent experiments. *p<0.05 between the indicated groups.

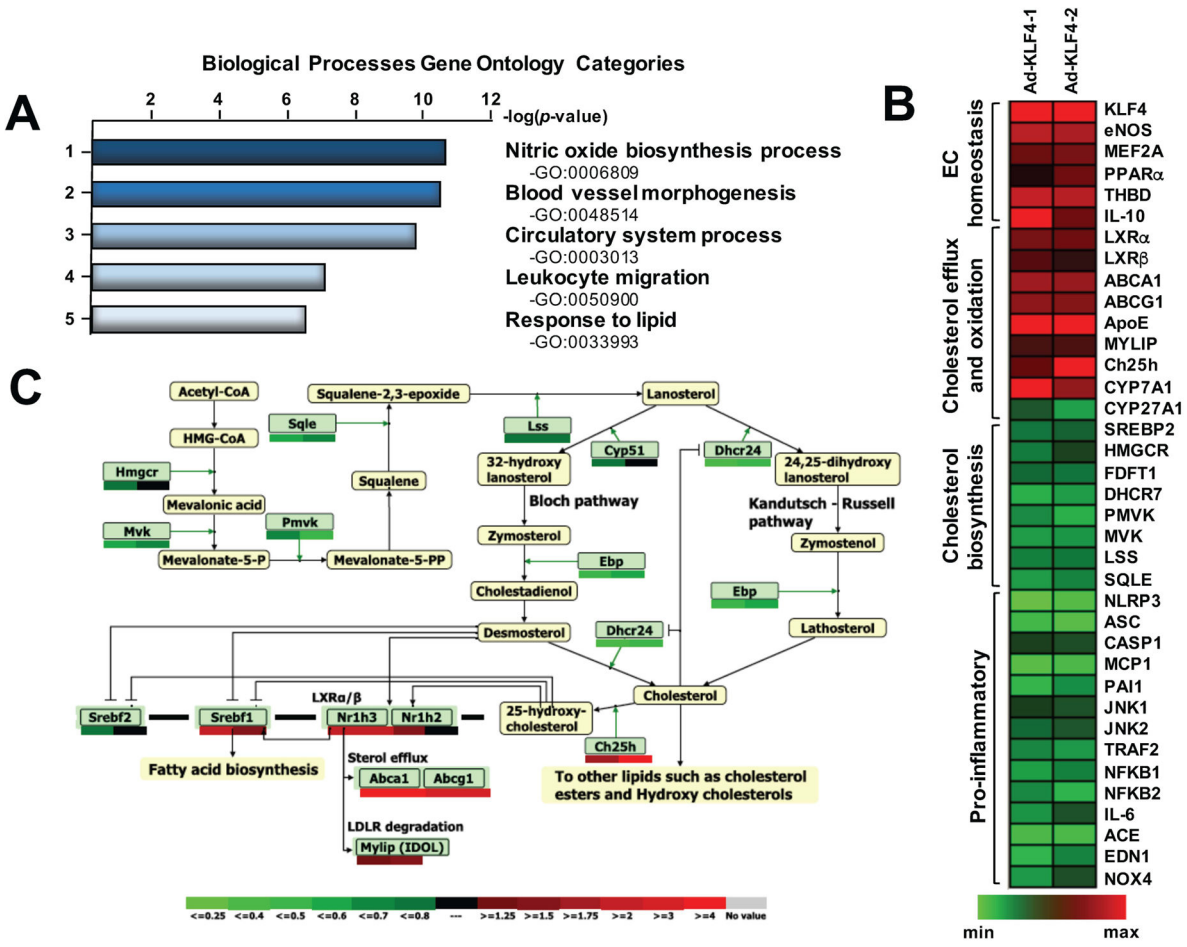

Figure 3. PS transcriptionally induces Ch25h

(A) WashU EpiGenome Browser depiction of the CpG islands and the binding landscape of H3K27ac, H3K4me1, H3K4me3, and Pol II at the promoter of the human *Ch25h* gene. The epigenetic landscapes shown were from HUVECs without stimulation. **(B–D)** HUVECs were subjected to PS or OS for 12 hr. **(E–G)** HUVECs were infected with Ad-KLF4 or Ad-null for 24 hr. In (B, E), DNA methylation status of the *Ch25h* promoter was measured by methylation-specific (MSP) qPCR. In (C, D, F, G), the binding of H3K4me3 and H3K27ac at the *Ch25h* promoter was detected using histone-ChIP qPCR. IgG was used as an isotype control. **(H–K)** Intima was collected from the AA or TA regions of C57BL/6 mice (n=9). In (H), total mRNA was quantified by qPCR. DNA methylation status is shown in (I). The modifications of H3K4me3 and H3K27ac are revealed in (J, K). Data presented are mean ±SEM from three independent experiments. *p<0.05 between the indicated groups.

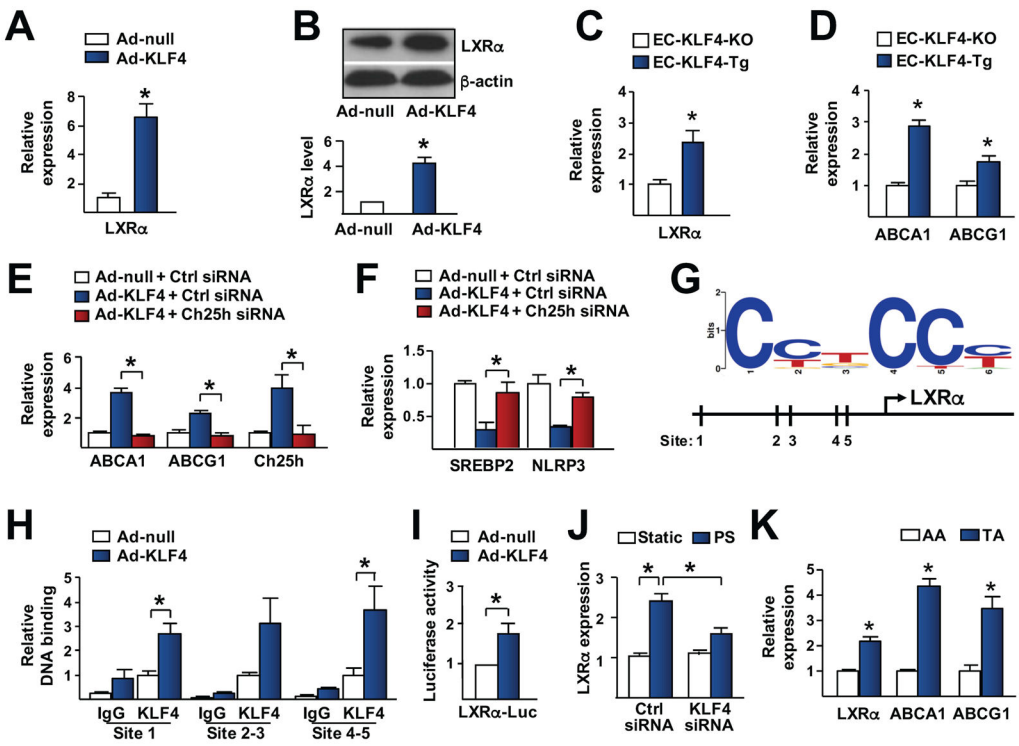

Figure 4. KLF4 transactivates LXRα

(A, B) HUVECs were infected with Ad-null or Ad-KLF4. Expression levels of LXRα mRNA (A) and protein (B) were measured by qPCR and Western blot, respectively. **(C, D)** The mRNA level of LXRα, ABCA1, and ABCG1 in lung ECs isolated from EC-KLF4-KO or EC-KLF4-Tg mice (n=3 per group) was detected by qPCR. **(E, F)** HUVECs infected with Ad-null or Ad-KLF4 were transfected with control siRNA or Ch25h siRNA. The level of ABCA1, ABCG1, Ch25h, SREBP2, and NLRP3 mRNA was assessed by qPCR. (**G**) Depiction of the predicted KLF4 binding sites at −3643 to 3632 bp (Site 1), −419 to −408 bp (Site 2), −313 to −302 bp (Site3), −219 to −208 bp (Site 4) and −133 to −122 bp (Site 5) in the human *LXRα* promoter region. **(H)** HUVECs were infected with Ad-null or Ad-KLF4 followed by ChIP assays using anti-KLF4. IgG was used as an isotype control. (**I**) BAECs were transfected with LXRα-Luc together with pRSV-β-gal reporter plasmids followed by infection with Ad-KLF4. Luciferase activity was measured and normalized to that of β-gal. (**J**) HUVECs were transfected with control siRNA or KLF4 siRNA followed by stimulation with PS or kept under static conditions for an additional 24 hr. (**K**) Intima was collected from the AA or TA regions of C57BL/6 mice (n=9). The mRNA expression of LXRα, ABCA1, and ABCG1 were measured by qPCR. Error bars represent mean±SEM from three independent experiments. *p<0.05 between the indicated groups.

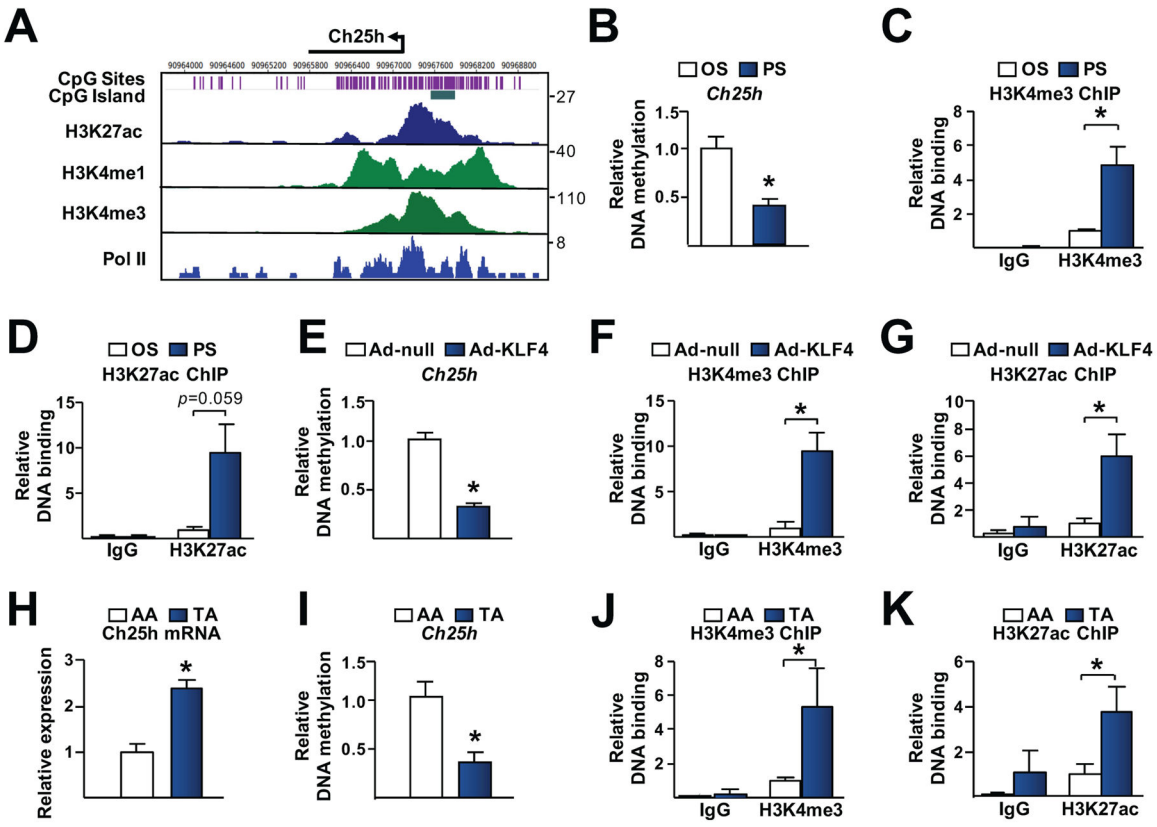

Figure 5. KLF4 regulation of Ch25h/LXR in macrophages promotes M2 polarization

(A) RAW264.7 cells were infected with Ad-KLF4 or Ad-null prior to qPCR assessment of the indicated mRNA. **(B)** LC-MS/MS measurement of intracellular 25-HC level of THP1 cells infected with Ad-KLF4 or Ad-null. **(C)** BMDMs from C57BL/6 mice were treated with 25-HC (5 nM) for the indicated time points. The mRNA expression profiles were analyzed by microarray as described in Shibata et al., 2013. The heat map shown indicate values plotted as relative fold change, compared with those from untreated controls. **(D, E)** RAW264.7 cells were treated with 25-HC (1 μM) or DMSO for 24 hr (D) or transfected with Ch25h siRNA or control siRNA (E). The mRNA levels of pro-inflammatory genes (NLRP3, IL-1β), M1 marker genes (COX2, Gro1, TNFα, CCL5, iNOS, and IL-6), and M2 marker genes (PPARγ, MRC, Chil3, Arg1, Retnla, and IL-10) were measured by qPCR. **(F–I)** PMs were isolated from 8-week old $Ch25h^{-/-}$ mice and their $Ch25h^{+/+}$ littermates (n=12 per group). The mRNA levels of the indicated genes were quantified by qPCR (F, I). In (G, H), the total cholesterol content and cholesterol efflux were measured. **(J)** PMs isolated from 8-week old $Ch25h^{-/-}$ mice (n=12) were treated with or without 25-HC (1 μM) for 24 hr. The mRNA levels of indicated genes were measured by qPCR. Error bars represent mean±SEM from three independent experiments. *p<0.05 between indicated groups.

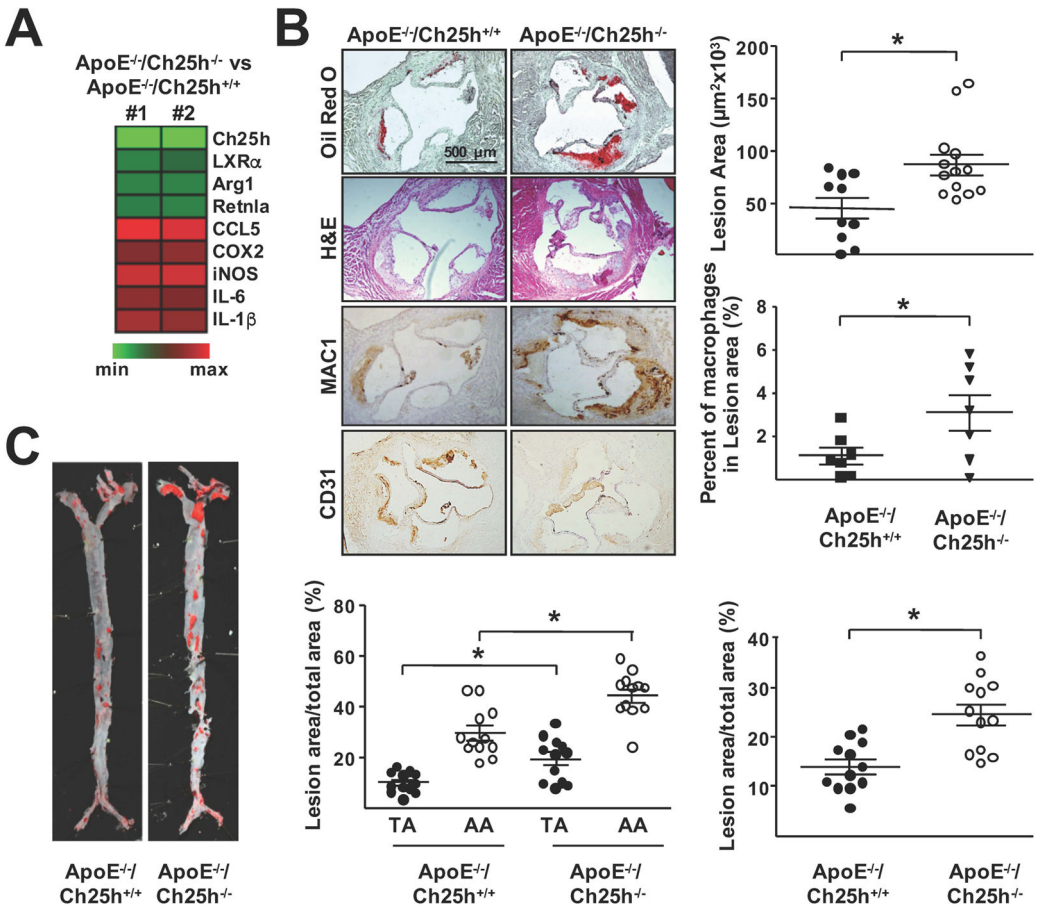

Figure 6. Ch25h ablation increases atherosclerosis susceptibility

(A) Two biological replicates of RNA-seq performed on PMs isolated from ApoE$^{-/-}$/Ch25h$^{-/-}$ compared to ApoE$^{-/-}$/Ch25h$^{+/+}$ mice (n=12 per group). Heat map is plotted as log2 fold change (refer to Figure S11 for heat map of scaled Z-score). **(B)** Six week-old ApoE$^{-/-}$/Ch25h$^{+/+}$ (n=13) and ApoE$^{-/-}$/Ch25h$^{-/-}$ (n=13) mice fed a high-fat diet for 12 weeks. Histological sections of aortic roots were stained with Oil Red O, H&E, MAC1, and CD31. Graphs on the right represent quantification of the Oil Red O-positive areas and percentage of macrophages in the lesions. **(C)** Representative *en face* Oil Red O staining of the whole aorta from ApoE$^{-/-}$/Ch25h$^{-/-}$ mice and ApoE$^{-/-}$/Ch25h$^{+/+}$ littermates (n=10 per group). Graphs on the right represent quantification of the lesion area in thoracic aorta (TA) versus aortic arch (AA) as well as total lesion area, summed from that of AA (i.e., aortic root, ascending aorta, and descending thoracic aorta to the 4th thoracic vertebra), TA (i.e., descending aorta from the 4th thoracic vertebra to the renal arteries), and abdominal aorta (i.e., below the renal arteries). Error bars represent mean±SEM from three independent experiments. *p<0.05 between the indicated groups.

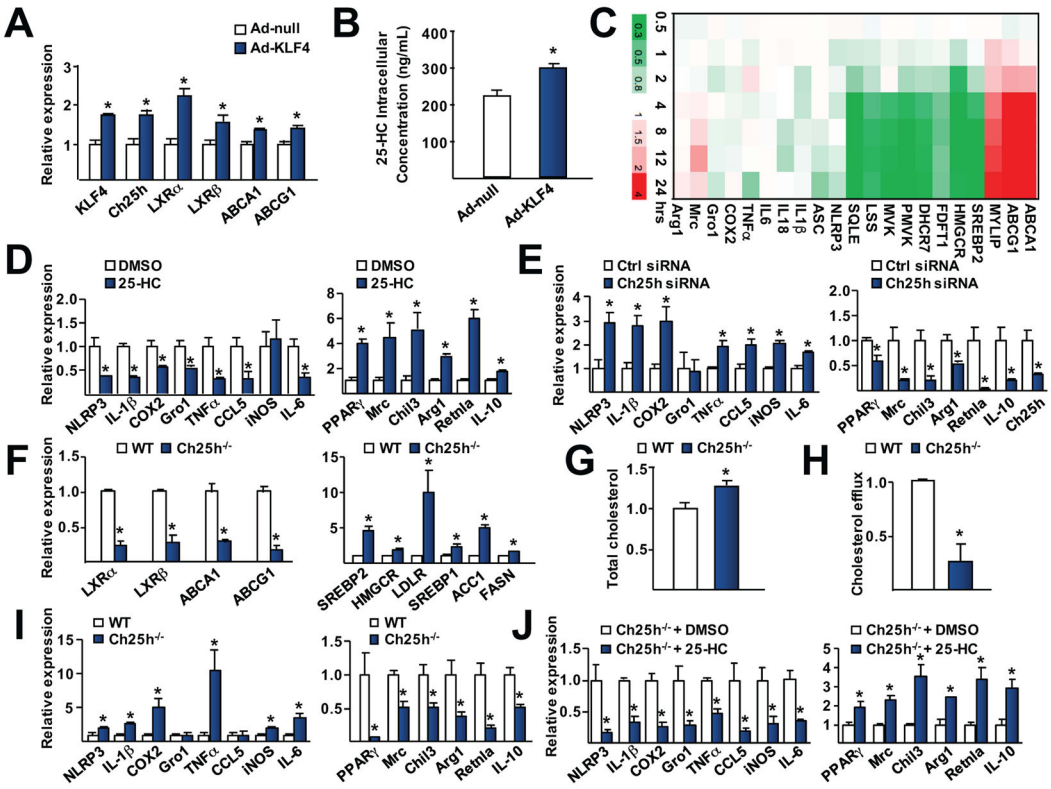

Figure 7. KLF4 mediates Ch25h and LXR in ECs and macrophages to promote a atheroprotective phenotype

Atheroprotective factors, such as pulsatile shear stress (PS) and statins, induce KLF4 in ECs and macrophages. KLF4 then transactivates Ch25h and LXR thereby promoting the suppression of SREBP2 and NLRP3 inflammasome in ECs as well as promotes cholesterol efflux and M1 to M2 transition in macrophages. The synergism between the anti-inflammatory effects in both ECs and macrophages contributes to the atheroprotective phenotype.